LA-UR-99-4175
Approved for public release; distribution is unlimited.

Title:

THE CHANGE IN THE MECHANICAL PROPERTIES OF ALLOY 718, 304L AND 316L STAINLESS STEEL AND AL6061 AFTER IRRADIATION IN A HIGH ENERGY PROTON BEAM

Author(s):

S.A. Maloy, M.R. James, W.F. Sommer, P. Ferguson, G. Willcutt, D. Alexander, M.R. Louthan Jr., M.L. Hamilton L. Snead and M.A. Sokolov

Submitted to:

http://lib-www.lanl.gov/cgi-bin/getfile?00796921.pdf

THE CHANGE IN THE MECHANICAL PROPERTIES OF ALLOY 718, 304L AND 316L STAINLESS STEEL AND AL6061 AFTER IRRADIATION IN A HIGH ENERGY PROTON BEAM

S.A. Maloy, M.R. James, W.F. Sommer, P. Ferguson, G. Willcutt, APT/TPO
D. Alexander, CMS
Los Alamos National Laboratory, Los Alamos, NM 87545

M.R. Louthan Jr., Westinghouse Savannah River Company, Aiken, SC 29808

M.L. Hamilton
Pacific Northwest National Laboratory, Richland WA 99352

L. Snead, M.A. Sokolov
Oak Ridge National Laboratory, Oak Ridge, TN 37831

ABSTRACT

The tensile properties and fracture toughness of age-hardened Alloy 718, annealed 304L and 316L stainless steel, and Al6061 in the T4 and T6 conditions have been investigated after irradiation at the LANSCE (Los Alamos Neutron Science Center) accelerator (800 MeV, 1mA) to a maximum dose of 12 dpa at temperatures from 30-200°C. Initial results show a degradation in toughness and a concomitant decrease in the uniform elongation with increasing proton and neutron fluence. The data are compared to the large database on radiation effects on the mechanical properties of structural materials exposed to fission reactor environments and show that many trends are similar. Additional data show that irradiation-induced reductions in uniform elongation are significant over dose/temperature ranges not anticipated from the fission reactor data. Hydrogen production through transmutation reactions and a susceptibility to hydrogen embrittlement may play key roles in the present low-temperature, low-dose degradation of mechanical properties.

1. INTRODUCTION

The Accelerator Production of Tritium (APT) Project is part of the US-DOE strategy to meet the nation's tritium (^{3}H) needs in the 21st century. Design, construction and operation of this one-of-a-kind facility will involve the utilization of a wide variety of materials that are exposed to unique conditions, including high-energy mixed proton and neutron spectra. The target/blanket portion of the APT system will contain components and structures with design lifetimes ranging from approximately one to over forty years. Component replacement schedules must be established to assure that operative material degradation processes do not compromise the safety and/or functionality of the system. Because of the unique exposure conditions associated with significant portions of the APT, the amount of experimental data that directly supports design lifetime determinations and replacement schedules is minimal. To correct this situation, a comprehensive materials test program has been established by the APT Project. This program includes the irradiation of structural materials by exposure to high energy protons and neutrons with the LANSCE accelerator. The proton flux produced in LANSCE is nearly prototypic of anticipated conditions for significant portions of the APT target/blanket system. Elements of the irradiation program include the determination and/or evaluation of:

- the effects of prototypical particle irradiation on the mechanical properties of Alloy 718, Types 304L and 316L stainless steels, 6061 aluminum and other candidate structural alloys,
- the corrosion behavior of the candidate structural materials under anticipated APT exposure conditions,
- tritium containment in the target/blanket system,
- microstructural evolution in materials exposed to anticipated APT proton and neutron spectra and fluxes, and
- material damage processes and mechanisms that will be operative in the APT system in view of the large production of H and He.

The materials program includes testing of base metals and cross-weld samples. The initial results from the program to establish the effects of a high-energy proton/neutron particle flux on the mechanical properties of base metal samples from Alloy 718, Types 304L and 316L stainless steels and 6061 aluminum are described below.

2. BACKGROUND

The APT Project will produce tritium through the ^{3}He(n,p)^{3}H reaction. The ^{3}He used for ^{3}H production will be contained, at approximately 130-260 psi, in 6061-T6

aluminum pressure tubes that will be connected to a $^{3}H/^{3}He$ separation facility through a Type 316L stainless steel manifold. Neutrons for the $^{3}He(n,p)^{3}H$ reaction will be produced by proton induced spallation of a tungsten target. Lead blanket assemblies will moderate and multiply the neutrons produced by spallation. The high energy proton beam that induces spallation in the tungsten target will move from the accelerator portion of the APT system into the target/blanket system by passing through an Alloy 718 window. Design concepts for the target/blanket system are summarized in Reference 1 and include cladding of the tungsten target elements and containment of the target cooling water with Alloy 718 and cladding the lead blanket components with 6061-T6 aluminum. The containment vessel will be fabricated from Type 304L stainless steel, and Type 316L stainless steel will be used to fabricate much of the primary cooling water system. The materials irradiation program developed to support the emerging target/blanket design is outlined in Reference 2, and, for convenience, is summarized in the next few paragraphs.

The proton beam used at LANSCE had a Gaussian-like intensity profile with a diameter of approximately $2\sigma = 3.0$cm, where σ is the standard deviation. The beam profile has two basic effects on the irradiation and specimen design:

- the specimen had to be small to assure reasonable uniformity in dose within a single sample, and
- placement of several specimens within a sample capsule provided the opportunity to determine the effects of dose on a given material.

The specimen also had to be relatively thin, 0.25 to 2.0 mm, to assure sufficient heat transfer to the coolant from the energy deposited by the 800 MeV proton beam. A schematic of sample placement in an irradiation sandwich or capsule is shown in Figure 1(top) and photographs of actual capsules are shown in Figure 1(bottom). The materials matrix is summarized in Table 1. The materials irradiation/test/analysis program was designed to provide information establishing the technical and scientific basis to:

1. determine the applicability of data trends established through fission reactor irradiation to predict irradiation effects on the mechanical properties of materials in spallation neutron sources,
2. establish anticipated materials' failure modes in spallation neutron sources and set maintenance schedules and system design lifetimes to avoid such failure modes,
3. understand the materials damage/degradation processes under anticipated irradiation/exposure conditions,

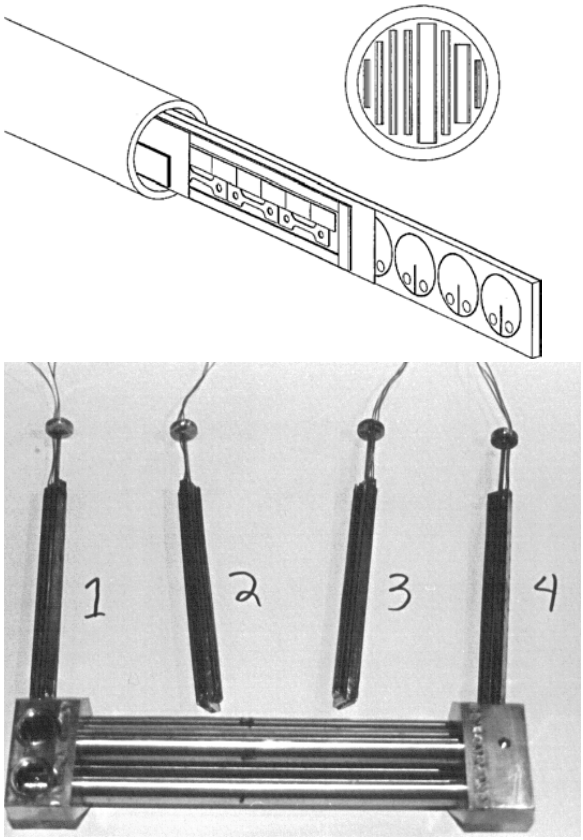

Figure 1. Capsules for Irradiation of Mechanical Test Samples. On top is the schematic of the test capsule and on bottom is a photograph of a test capsule

4. model irradiation effects in spallation neutron sources, and
5. extrapolate materials behavior into new damage arenas and/or select alternate materials for APT service.

In addition, prototypes of the tungsten neutron source and the lead/aluminum blanket have been irradiated with 800 MeV protons and spallation neutrons at power levels prototypic of the power levels anticipated in the APT target.

This paper summarizes the initial test results from samples of Alloy 718, 6061 aluminum and Types 304L and 316L stainless steel irradiated in the LANSCE to approximately 0.5 to 12 dpa. The measured tensile and fracture toughness data are compared to fission reactor data to show that, under the test conditions evaluated, fission reactor data provide useful indicators of anticipated materials behavior in spallation neutron sources except at higher doses where H and He effects are anticipated.

Table 1. Material Test Matrix

Material	Tensile Tests	Fracture Toughness Tests	TEM/Shear Punch Tests	3 pt. Bend tests
Alloy 718 (precipitation hardened)	X	X	X	X
304L (annealed)	X	X	X	X
316L (annealed)	X	X	X	X
Al6061-T6	X	X		X
Al6061-T4	X		X	X
Mod 9Cr-1Mo	X	X	X	X
Al5052-O	X	X	X	X
Tungsten (wrought)			X	
Lead			X	

Table 2. Chemical Composition of Materials Tested

Material	Al	C	Cr	Cu	Fe	Mn	Mo	Ni	P	S	Si	Ti	Others
Alloy 718 2-4 mm	0.47	0.04	17.71	0.15	BAL	0.12	3.00	54.79	0.013	0.001	0.13	0.98	Nb and Ta-4.98; Co-0.19; B-0.002
Alloy 718 0.25 mm	0.48	0.04	18.13	0.08	BAL	0.13	3.06	53.58	0.008	0.001	0.11	1.03	Nb and Ta-4.98
Alloy 718 0.75 mm	0.54	0.05	18.13	0.05	BAL	0.21	3.01	52.7	0.005	0.002	0.13	1.06	Nb and Ta-5.07; Co-0.4; B-0.004
316L 2-4 mm		0.010	17.33	0.18	BAL	1.61	2.09	10.62	0.024	0.019	0.43		Co-0.21; N-0.060
316L 0.25 mm		0.019	17.26	0.26	BAL	1.75	2.57	12.16	0.022	0.006	0.65		
316L 0.75 mm		0.022	16.05		BAL	1.82	2.08	10.11	0.022	.0002	0.48		
304L 2-4 mm		0.013	18.15	0.23	BAL	1.80	0.18	8.35	0.025	0.010	0.43		Co-0.17, N-0.085
304L 0.25 mm		0.020	18.23	0.38	BAL	1.77	0.33	9.68	0.026	0.002	0.54		
304L 0.75 mm		0.060	18.19	0.4	BAL	1.86	0.34	8.14	0.030	.0003	0.48		
Al6061 0.25 mm	Bal.		0.04/ 0.35	0.15/ 0.4	0.70 Max	0.15 Max					0.40/ 0.80		Mg-(0.8-1.2); Zn-0.25
Al6061 0.75 mm	Bal		0.04/ 0.35	0.15/ 0.4	0.70 Max	0.15 Max					0.40/ 0.80	0.15 Max	

3. MATERIALS SPECIFICATIONS AND HEAT TREATMENT

Certified mill test reports were obtained for each alloy; the chemical composition, from these test reports, for each material is summarized in Table 2. Three heats of each alloy were tested; one heat for specimens 0.25 mm thick, one heat for specimens between 0.75 and 1.0 mm thick, and another heat for specimens between 2.0 and 4.0 mm thick.

Alloy 718 specimens were machined from the as-received material (annealed condition), wrapped in Nb foil and encapsulated in a quartz tube (evacuated and back-filled with Ar). The encapsulated specimens were heat treated through the following steps:

- Anneal at 1065°C for 30 minutes and air cool,
- Age at 760°C for 10 hours,

- Furnace cool from 760°C to 650°C and hold for a total time of 20 hours,
- Air cool to room temperature.

The 316L and 304L stainless steel samples were machined (EDM) from as-received (annealed) material and irradiated in the as-machined and cleaned condition and tested after irradiation.

The 6061 Al samples were ordered as 6061-T6 and were irradiated in the as-received condition and then tested after irradiation. Hardness and transmission electron microscopy measurements on the control samples demonstrated that some of the materials had not been heat treated to the T6 condition but were actually in the T4 condition. Therefore, the 6061 Al irradiation included samples in the T6 and the T4 conditions.

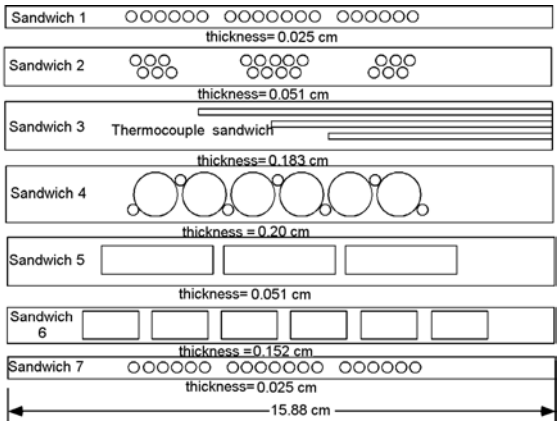

A.

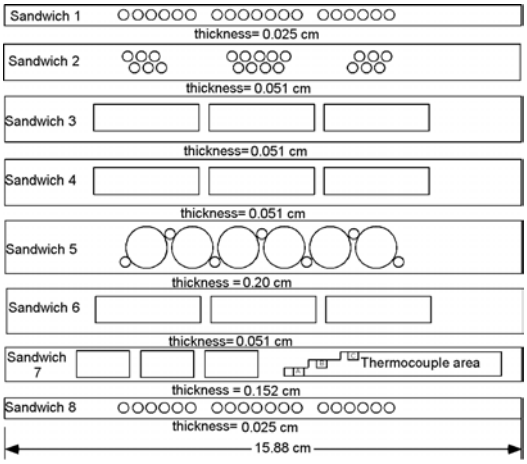

B.

Figure 2. Arrangements of Specimen Sandwiches with-in Sample Tubes

4. IRRADIATION PROCEDURES AND TEMPERATURE AND DOSE CALCULATIONS

Specimens were irradiated in specially designed sandwiches to control the specimen irradiation temperature and isolate the specimens from the water coolant. Each sandwich included a holder to position and space the specimens within the tube and two 0.25 mm thick cover plates which were TIG welded to each side of the holder. The holder and the cover plates were fabricated from Type 304L stainless steel. Two different sandwich arrangements were irradiated as shown in Figure 2.

Each arrangement held similar types of specimens but had a slightly different thermocouple arrangement to measure irradiation temperature. For example, sandwich 3 in arrangement A contained three thermocouples with tips spaced 2 cm apart and the center thermocouple was in the center of the sandwich. Sandwich 7 in arrangement B held tensile samples, bend samples and three thermocouples brazed in metal pads. The other sandwiches, in both arrangements, contain a variety of tensile, compact tension samples, bend samples, transmission electron microscopy disks and activation foils. The activation foils were selected to provide the technical basis to estimate dose and support the model calculations based on the LCS (LAHET Code System) This system couples the Los Alamos High Energy Transport (LAHET) code with Monte Carlo for Neutrons and Photons (MCNP) code.

Irradiation temperatures were determined by considering:

- thermocouple measurements in one sandwich from each tube,
- physics calculations (using the LAHET code) of the power densities in each location, and
- measurement of the cooling water temperatures and flow rates through each tube.

This information was combined to determine a gap resistance to heat transfer from the irradiated samples to the cover plates and then to calculate specimen irradiation temperatures based on the calculated power density, cooling conditions and the gap resistance. A detailed description of this analysis is found in Reference 3. Irradiation temperatures were between 30 and 200°C, depending on sample thickness, sample position in the tube, and tube position relative to the proton beam.

Detailed modeling of the irradiation, carried out using the LAHET code system, was based on the configuration of the specific inserts exposed to the proton beam. A schematic of the insert arrangement (inserts 17A, 18A, 18B, etc.) is shown in Figure 3. Insert 18A, for example, contained models of the tungsten target assemblies and produced the neutrons which irradiated the test samples

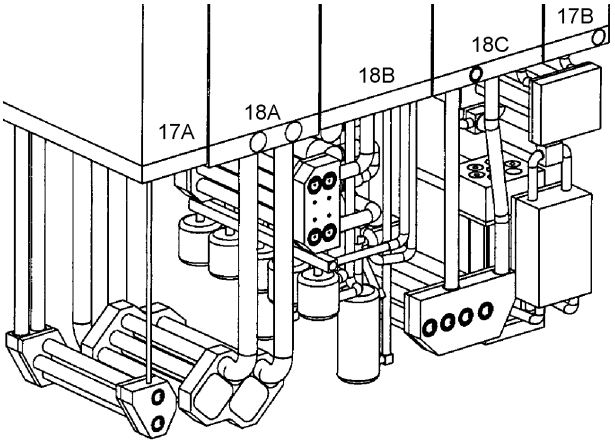

Figure 3. Schematic of Inserts and Associated Sample Tubes

contained in the other inserts. The mixed proton/neutron spectrum varied with position in the test matrix and was relatively prototypic of anticipated APT conditions for various portions of the target/blanket system. Modeling of the sample tubes was done by placing the cooling water, cover plates and sample material in separate regions in each tube. Calculations of proton flux, neutron flux, dpa, He/H production and energy deposition were performed for sample tubes in 17A, 18A, and 18C.

The fluence determination for the irradiated samples was performed through analysis of the activation foils that were irradiated in each sample tube(4). The activation foil packages were TEM-sized disks punched from >99.98% pure sheet material of Al, Fe, Co, Ni, Cu, and Nb. The disks were placed together in stacks and irradiated in the sample tube. After irradiation, the stacks were withdrawn and counted with gamma spectroscopy to quantify the isotopes produced. This provided several reactions with various cross sections and thresholds which were used to estimate the proton and neutron group fluxes. The production rates of the isotopes were calculated by taking into account the proton beam history and the measured activity. Proton and neutron flux estimates were calculated using the LAHET Code System and a model of the irradiation target. The input fluxes were then adjusted to match the measured isotope production rates using the STAYSL2 code. The revised fluxes for protons and neutrons were then folded with He, H and dpa cross sections for the materials of interest. This firmly established the exposure parameters at the activation foil locations. Assignment of exposure values to the samples necessitated interpolation between the activation foils. The was done by curve fitting, usually one or more Gaussians, to the exposure parameters (proton fluence, dpa, etc.) and using the mathematical equation for the interpolation. The error associated with the fluxes and damage levels was estimated to be around 25%, but in gas production, where larger systematic errors were known to exist in the cross sections, errors may be larger. Measurements of the gas content of samples following irradiation are being used to better determine H and He production crossections (5)

5. TEST RESULTS

Type 304L and 316L Stainless Steel

The tensile samples, both the irradiated and non-irradiated control samples, were tested at 20, 50, 80 and 164°C. The test temperatures corresponded approximately to the irradiation temperatures. The irradiation temperature decreased, as did the particle fluence, with distance from the proton beam. Therefore, those samples irradiated closest to the center of the beam were heated to the highest temperatures, experienced the highest dpa values and were tested at the highest temperature. Separation of the effects of the irradiation and test temperature from the effects of irradiation per se was not attempted directly, however, data are discussed in terms of the effects of dpa and/or temperature on the various measured mechanical properties.

The tensile test data for the Type 316L and Type 304L specimens are summarized in Figures 4-7. In general, the data trends are similar to the previously reported effects of low temperature neutron irradiation on the tensile properties of austenitic stainless steel (6). The irradiation increased the strength and decreased the ductility of both types of steel. The yield strength increases rapidly with dpa and reaches a maximum of 850 MPa in Type 316L samples irradiated to approximately 10 dpa and tested at 164°C. This maximum is consistent with the observation

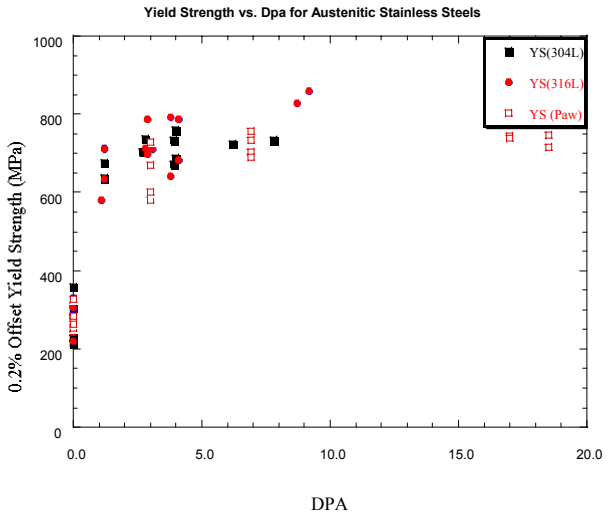

Figure 4. Effect of Irradiation Dose, dpa, on the Yield Strength of Austenitic Stainless Steels. Open data points are from Figure 1 in Reference 7 and were for samples irradiated in HFIR and tested at 25 to 250°C. Closed points are for samples irradiated in a high energy proton and neutron spectrum.

that fission irradiation-induced hardening in a number of austenitic stainless steels, irradiated and tested at 25 to 250°C, causes the yield strength to saturate at 900 MPa, or less, by 3 to 7 dpa (7). Additionally the increases in yield strength caused by irradiation in the spallation-induced mixed proton/neutron spectra are consistent with the effect of fission reactor neutron dose on yield strength, Figure 4.

The irradiation-induced strength increases were accompanied by a loss in work hardening ability and a premature onset of plastic instability, Figure 5. The lack of work hardening in the austenitic matrix causes a significant reduction in the ability of the alloy to experience uniform elongation, Figure 6. These effects are attributed to irradiation-induced changes in microstructure which include the formation of interstitial and vacancy loops and the development of black spot damage associated with nanometer size vacancy and interstitial clusters (8,9). The loops and clusters act as barriers to dislocation motion and strengthen the austenite lattice. The first dislocations to pass through the defected microstructure disrupt and reduce the strength of the dislocation barriers. This disruption reduces the stress required to move the next group of dislocations along the same path or channel. The onset of dislocation channeling has been used to explain the irradiation induced yield drop and the loss of work hardening (8). Without work hardening, strain becomes localized to the regions of initial dislocation movement and, in the extreme, most of the dislocation motion is confined to the initial channel. In such cases, failure will ultimately occur in the region of dislocation channeling. The failure will be macroscopically brittle (no significant uniform elongation) even though the failure processes were entirely ductile. The temperature-dpa region corresponding to an almost-complete loss of uniform elongation was broader for the samples irradiated in the high energy mixed proton/neutron spectra than the range reported in Reference 8 for samples irradiated by neutrons in a reactor, Figure 7. Inclusion of the data from this study expanded the "embrittlement" range to both lower test temperatures and lower doses. The expansion may be attributed to the hydrogen (and perhaps helium) content in the samples tested in this study.

Radiation damage in materials exposed to high energy mixed proton/neutron spectra typical of the APT target/blanket region will include the production and implantation of greater quantities of hydrogen and helium than typically found in materials exposed to fission reactors. High hydrogen concentrations promote strain localization in metals and alloys tested at near ambient temperatures (10,11). Such localization is one of the postulated mechanisms for hydrogen embrittlement and has been associated with the observation that the fracture processes in many "hydrogen embrittled" materials show evidence of large-scale, localized plasticity (12), even when the elongation-to-fracture is minimal. The tendency for irradiation-induced dislocation channeling in austenitic alloys may combine with hydrogen induced strain localization to further decrease the ability of the

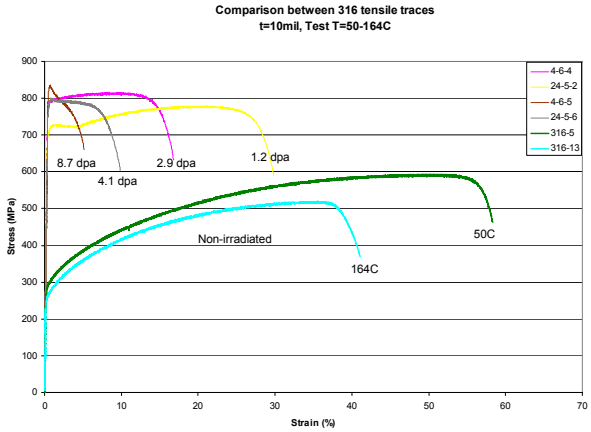

Figure 5. Stress-Strain for Irradiated and Non-irradiated Type 316L Stainless Steel Samples Tested at 50 and 164°C.

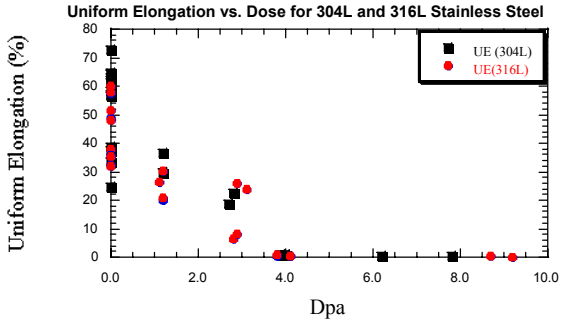

Figure 6. Effect of Dose on Uniform Elongation in Austenitic Stainless Steel Samples Irradiated in High-Energy, Mixed Proton/Neutron Beam

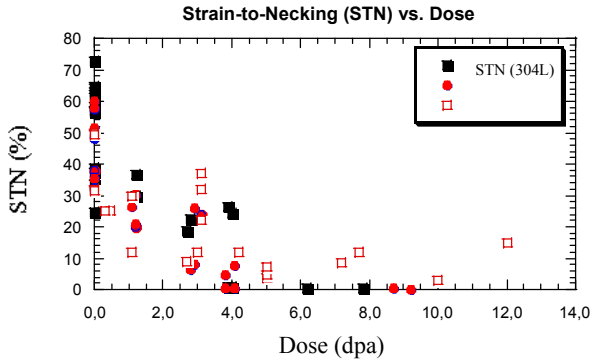

Figure 7 Strain-to-Necking as a Function of Dose and Temperature for Austenitic Stainless Steels. Open data points are from Figure 4 in Reference 6 and were for samples irradiated by neutrons in a reactor. Closed points are for specimens irradiated in a high energy proton and neutron flux.

steel to work harden. The tendency for hydrogen induced strain localization will increase as the test temperature decreases from 200°C toward room temperature. Therefore, the observation that the low temperature loss in uniform elongation is greater in austenitic stainless steels irradiated under conditions typical of high energy spallation neutron sources than in reactor irradiated austenitic stainless steel is consistent with onset of established hydrogen embrittlement processes. This consistency supports the conclusion that hydrogen production in spallation neutron sources will enhance the effects of displacement damage and promote losses in uniform elongation at temperature/dpa conditions lower than anticipated from fission reactor data. Recent hydrogen and helium measurements on irradiated materials from this same LANSCE irradiation show high hydrogen and helium retention in 304L and 316L after irradiation to 4 dpa (13). This possibility has been previously suggested during an evaluation of potential damage problems in high power spallation neutron sources (14). A similar effect of hydrogen and helium implantation was also observed in measurements of the fracture toughness of these same austenitic stainless steels.

Irradiation decreased the fracture toughness of Type 304L and 316L stainless steel, Figure 8. This decrease, at low doses, was slightly greater than the equivalent behavior for reactor-irradiated, austenitic stainless steels (15). For example, low temperature irradiation (70 to 155°C) of Type 304 and 316 stainless steel to 2-3 dpa lowered K_{jc} fracture toughness values by 15 to 30% (15) while the K_{jq} fracture toughness values of samples irradiated in this study were reduced approximately 50% after similar exposures. This increased loss in toughness is consistent with the observation that both hydrogen and hydrogen/helium accumulations lower the room temperature fracture toughness of austenitic stainless steels (16). Additionally, the irradiation-induced loss in toughness appears to saturate at doses slightly less than 10 dpa, the dose required for saturation in reactor irradiated steels. However, the measured saturation toughness values, K_{jq} = 50 to 100 MPa $m^{½}$, are similar to the saturation toughnesses previously found for reactor irradiated steels, K_{jc} = 40 to 70 MPa $m^{½}$. Little significance should be placed on the observation that, for the two heats of steel irradiated in this study, Type 304L showed a higher value of saturation toughness than did Type 316L. Heat-to-heat variations in the fracture toughness of austenitic stainless steels are quite large and have been correlated with variations in inclusion size, shape and distribution (15). Metallographic studies showed that the heat of Type 316L steel tested in this study contained more inclusions than the heat of Type 304L steel tested, an observation consistent with the trend

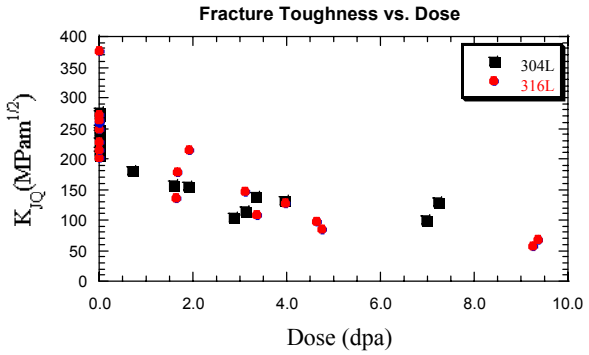

Figure 8. Effect of Dose on Fracture Toughness of Austenitic Stainless Steels Irradiated in High Energy, Mixed Proton/Neutron Spectra

for high inclusion contents to lower fracture toughness values.

These initial mechanical property measurements on Type 304L and Type 316L stainless steel samples irradiated in high energy, mixed proton/neutron spectra demonstrate that fission reactor data can be used to predict trends in behavior. The data also indicate that, between 25 and 200°C, the displacement damage effects are enhanced by the presence of transmutation products such as hydrogen. This enhancement decreases the dpa required to cause a specific change in a mechanical property but does not significantly impact the saturation values in that property. However, the lack of apparent impact of spallation products on saturation values may not extrapolate to higher irradiation/test temperatures and/or higher exposure levels.

Alloy 718

Heat treatment of the Alloy 718 produced an alloy having a yield strength of approximately 1200 MPa. This strength level was primarily due to the presence of metastable γ' ($L1_2$ structure) and γ" (DO_{22} structure) precipitates in the austenite lattice (17). The γ" phase is generally considered the primary strengthening precipitate with the γ' providing only modest contributions to the overall strength. Irradiation had minimal effects on the strength but significantly decreased the ductility, especially uniform elongation, and toughness of the heat-treated Alloy 718, Figures 9-10. These radiation-induced changes in the mechanical properties were similar to the changes found in the 300 series steels, in that the trends were similar to those found from (very limited) fission reactor data (18-20), but apparently occurred at lower dpa levels. For example, neutron irradiation exposures over approximately 10 dpa reduced the fracture toughness of heat treated Alloy 718 by about 50% regardless of the initial non-irradiated toughness (19, 20). The irradiation-induced losses in toughness appeared to saturate after

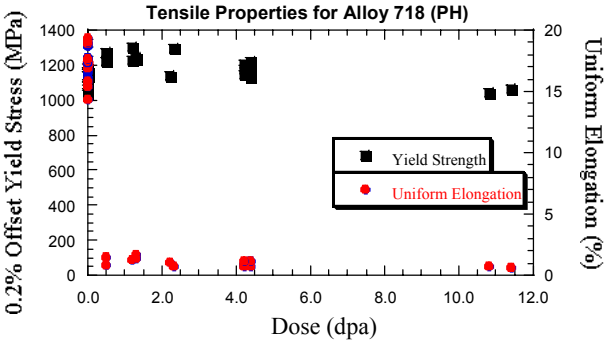

Figure 9. Effect of Dose on the Tensile Properties of Alloy 718 Irradiated in a High Energy Mixed Proton/Neutron Spectra

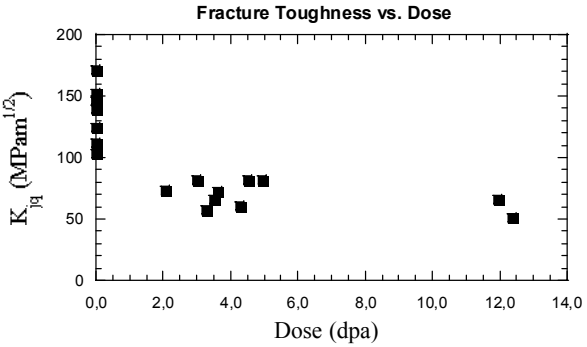

Figure 10. Effect of Dose on Fracture Toughness of Precipitation Hardened Alloy 718 Irradiated in a High Energy, Mixed Proton/Neutron Spectra

about 8 dpa. Similar reductions in toughness were found in this study after only 2 to 3 dpa. This difference is attributed to the increased helium and hydrogen production associated with irradiation in the high-energy, mixed proton/neutron exposures used for the present investigation and the susceptibility of Alloy 718 to hydrogen embrittlement at near ambient temperatures.

The lack of significant radiation-induced strengthening is attributed to the combination of softening caused by a loss of γ' and γ" precipitates and matrix hardening through the accumulation of displacement damage. Transmission electron microscopy of portions of an Alloy 718 beam window that had been irradiated by high energy protons to a maximum dose of approximately 10 dpa showed that the irradiation caused dissolution of the strengthening phases and formation of η (DO_{24} structure) phase precipitates (21). Microhardness measurements and bend test results demonstrated that radiation induced softening accompanied the disappearance of the strengthening phases (21). Additionally, the bend test samples also showed a transition in fracture mode from microvoid coalescence to intergranular as the radiation dose increased toward 10 dpa. A similar transition in fracture mode in Inconel 706 (an alloy derived from the Alloy 718 composition) has been associated with the appearance of η and δ (DO_a structure) phases (22). The formation of the η and δ phases in Alloy 718 is generally associated with overaging due to prolonged exposures at elevated temperature. Irradiation induced aging, however, apparently favors the formation of η over δ (23). Microstructural evolution toward these "overaged" structures will degrade the mechanical properties, irrespective of the effects of displacement damage and hydrogen/helium accumulation in the Alloy 718.

These initial measurements of the effects of high-energy, proton/neutron radiation on the mechanical properties of Alloy 718 are similar to the effects observed for austenitic stainless steels. The fission reactor data trends provide useful indications of property degradation but fail to predict the additive effects of gas production on degradation at low dose levels. At the low irradiation and test temperatures used in this study, hydrogen is considered to be the primary contributor to the more rapid degradation. Support for this conclusion was found in tests of 6061 aluminum samples from the same proton/neutron irradiation but exposed to lower doses.

6061 Aluminum

The 6061 alloy was irradiated in the T4 and T6 conditions to a maximum of 1.5 dpa. The tensile properties of samples that were in the T6 condition were relatively unaffected while the tensile properties of specimens in the T4 condition increased in strength and decreased in ductility with increasing dose, see Figs. 11 and 12. The increased strength and decreased ductility in the samples in the T4 condition are attributed to the effectiveness of the dislocation obstacles introduced by the displacement damage. The lack of change in the tensile properties of samples in the T6 condition is almost identical to the behavior previously observed for samples irradiated in

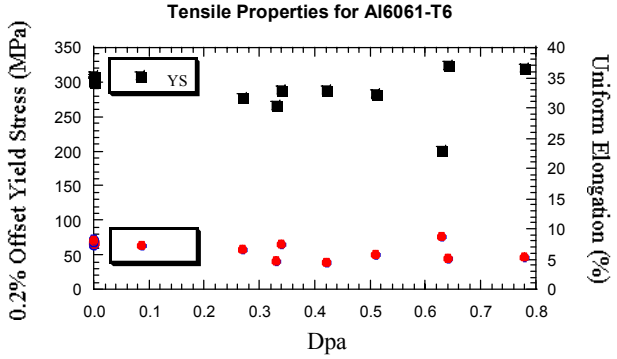

Figure 11. Effect of Dose on the Tensile Properties of Al6061-T6 Irradiated in a High Energy Mixed Proton/Neutron Spectra.

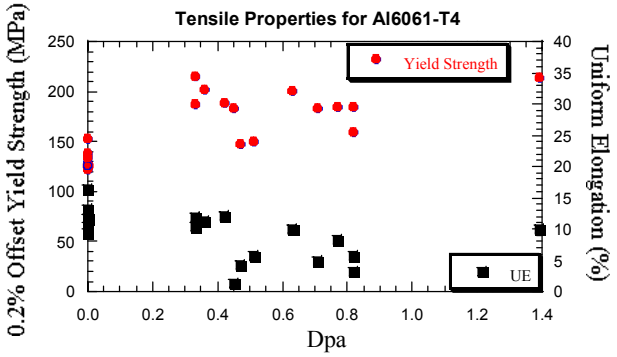

Figure 12. Effect of Dose on the Tensile Properties of Al6061-T4 Irradiated in a High Energy Mixed Proton/Neutron Spectra

fission reactors, even at the low dose levels where specimens were irradiated and tested at 50°C (24). This lack of additive effects due to the enhanced gas production in the high-energy proton/neutron environments is attributed to the lack of significant hydrogen embrittlement in the 6061 aluminum.

Conclusions

The data presented in this report demonstrate that the large data base of radiation effects on the mechanical properties of structural metals and alloys exposed to fission reactor environments provides useful indicators of the anticipated trends for property/dose predictions in spallation neutron environments. However, the enhanced gas production associated with the high-energy proton/neutron spectra in spallation neutron sources did cause enhanced degradation at low doses. Additionally, data show that irradiation-induced losses in uniform elongation are significant over dose/temperature ranges not anticipated from the fission reactor data. Hydrogen production, and a susceptibility to hydrogen embrittlement, may play key roles in the low temperature, low dose degradation. Clearly, additional data are required to confirm the postulated hydrogen effects and additional data at higher dose levels are required before the saturation levels for mechanical property degradation can be confirmed. The data necessary to provide such confirmations should be forthcoming from the APT materials test program. This report presents the initial results from an extensive, continuing irradiation effects program that will ultimately include the microstructural observations and corrosion data necessary to demonstrate the behavior of structural materials at low temperatures (30-200°C) in the radiation environments typical of spallation neutron sources.

Acknowledgments

This program benefited from a large collaboration involving scientists and engineers from numerous groups at Los Alamos National Laboratory as well as a materials working group consisting of representatives from Pacific Northwest National Laboratory, Oak Ridge National Laboratory, Sandia National Laboratories, Lawrence Livermore National Laboratory, Savannah River Technology Center, and Brookhaven National Laboratory. We are indebted to all participants.

References

1. M. W. Cappiello and A. M. Baxter, “APT Target/Blanket Design”, AccApp’98, pp. 289-296, American Nuclear Society, La Grange, IL, 1998.
2. S. A. Maloy, W. F. Sommer, R. D. Brown, J. E. Roberts, J. Eddleman, E. Zimmermann and G. Willcutt, “Progress Report on the Accelerator Production of Tritium Materials Irradiation Program”, Materials for Spallation Neutron Sources, edited by M. S. Wechsler, L. K. Mansur, C. L. Snead and W. F. Sommer, pp. 131-138, TMS, Warrendale, PA, 1998.
3. G.J. Willcutt, S.A. Maloy, M.R. James, J. Teague, D.A. Siebe, W.F. Sommer, P.D. Ferguson, “Thermal Analysis of the APT Materials Irradation Samples”, 2nd International Topical Meeting on Nuclear Applications of Accelerator Technology, Gatlinburg, TN, Sept. 20-23, 1998, pp. 254-259.
4. M.R. James, S.A. Maloy, W.F. Sommer, P. Ferguson, M.M. Fowler, K. Corzine, “Determination of Mixed Proton/Neutron Fluences in the LANSCE Irradiation Environment”, 2nd International Topical Meeting on Nuclear Applications of Accelerator Technology, Gatlinburg, TN, Sept. 20-23, 1998, pp. 605-608.
5. Oliver, B.M., Hamilton, M.L., Garner, F.A., Sommer, W.F., Maloy, S.A. and Ferguson, P.D., “Helium/Hydrogen Measurements in High-Energy Proton-Irradiated Tungsten”, Effects of Radiation on Materials, 19th International Symposium, ASTM STP 1366, M.L. Hamilton, A.S. Kumar, S.T. Rosinski, and M.L. Grossbeck, Eds., American Society for Testing and Materials, West Conshohocken, PA, 1999, in press.
6. , J.E. Pawel, A.F. Rowcliffe, G.E. Lucas, S.J. Zinkle, “Irradiation Performance of Stainless Steels for ITER Application”, vol. 239, J. of Nuclear Materials, pp. 126-131, 1996.
7. J. E. Pawel, A. F. Rowcliffe, D. J. Alexander, M. L. Grossbeck and K. Shiba, “Effects of Low Temperature Neutron Irradiation on the Deformation Behavior of Austenitic Stainless Steels” vol. 233-237, Journal of Nuclear Materials, pp. 202-206, 1996
8. J. E. Pawel-Robertson, I. Ioka, A. F. Rowcliffe, M. L. Grossbeck and S. Jitsukawa, “Temperature Dependence of the Deformation Behavior of 316 Stainless Steel after Low Temperature Neutron

Irradiation", pp. 225-238, ASTM STP 1325, R. K. Nanstad, M. L. Hamilton, F. A. Garner and A. S. Kumar, Eds., American Society for Testing and Materials, Philadelphia, 1997.
9. H. Ullmaier, "Radiation Damage in Metallic Materials", MRS Bulletin, pp. 14-23, Vol.22, Number 4, 1997.
10. J. P. Hirth and O. A. Onyewuenyi, in Environmental Degradation of Engineering Materials in Hydrogen, edited by M. R. Louthan, Jr., R. P. McNitt, and R. D. Sisson, Jr., Virginia Polytechnic Institute, Blacksburg, VA, 1981.
11. M. R. Louthan, Jr., "Strain Localization and Hydrogen Embrittlement", Scripta Metallurgica, pp. 451-454, Vol. 17, 1983.
12. J. P. Hirth, "The Role of Hydrogen in Enhancing Plastic Instability and Degrading Fracture Toughness in Steels", pp. 507-522, Hydrogen Effects in Materials, edited by A. W. Thompson and N. R. Moody, TMS, 1996.
13. Oliver, B., Garner, F.A., Maloy S.A., Sommer, W.F., and Ferguson, P.D., Proceedings of the Third International Conference on Spallation Materials Technology, Santa Fe, NM, April 29 - May 4, 1999, in preparation
14. H. Ullmaier and F. Carsughi, "Radiation Damage Problems in High Power Spallation Neutron Sources", Nuclear Instruments and Methods in Physics Research B, pp.406-421, Vol. 101, 1995.
15. W. J. Mills, "Fracture Toughness of Types 304 and 316 Stainless Steels and Their Welds", International Materials Reviews, pp. 45-82, Vol., 1997.
16. M. J. Morgan and M. A. Tosten, "The Effect of Tritium Decay Helium on the Fracture Toughness of Austenitic Stainless Steels", p. Hydrogen Effects in Materials, edited by A. W. Thompson and N. R. Moody, TMS, 1996.
17. M. Sundararaman, P. Mukhopadhyay and S. Bannerjee, "Precipitation and Room Temperature Deformation Behavior of Inconel 718", pp. 419-440, Superalloys 718, 625, 706 and Various Derivatives, edited by E. A. Loria, TMS, Warrendale, PA, 1994.
18. L. Ward, J. M. Steichen and R. L. Knecht, "Irradiation and Thermal Effects on the Tensile Properties of Inconel-718", pp. 156-170, ASTM STP 611, American Society for Testing and Materials, Philadelphia, 1976.
19. W. J. Mills, "Effect of Microstructural Variations on the Tensile and Fracture Toughness Properties of Alloy 718 Welds", pp. 845-858, Superalloys 718, 625, 706 and Various Derivatives, edited by E. A. Loria, TMS, Warrendale, PA, 1994.
20. D. J. Michel and R. A. Gray, "Effects of Irradiation on the Fracture Toughness of FBR Structural Materials", pp. 194-203, Vol. 148, Journal of Nuclear Materials, 1987.
21. F. Carsughi, H. Derz, P. Ferguson, G. Pott, W. Sommer and H. Ullmaier, "Investigations on Inconel 718 Irradiated with 800 MeV Protons", Journal of Nuclear Materials, pp. 78-88, vol. 264, 1999.
22. G. W. Kuhlman, A. K. Chakrabarti, R. A. Beaumont, E. D. Seaton and J. F. Radavich, "Microstructure – Mechanical Properties Relationships in Inconel 706 Superalloy", pp. 441-450, Superalloys 718, 625, 706 and Various Derivatives, edited by E. A. Loria, TMS, Warrendale, PA, 1994.
23. W. L. Bell and T. Lauritzen, "Microstructural Changes in Neutron-Irradiated Commercial Alloys: A Sequel", pp. 139-151, ASTM STP 782, H. R. Barager and J. S. Perrin, Eds., American Society for Testing and Materials, Philadelphia, 1982.
24. Farrell, K., "Response of Aluminum and its Alloys to Exposure in the High Flux Isotope Reactor", in Dimensional Stability and Mechanical Behaviour of Irradiated Metals and Alloys, British Nuclear Energy Society, London, Paper P11, 1983.